

Implicit handling of multilayered material substrates in full-wave SCUFF-EM calculations

Homer Reid

August 16, 2017

Contents

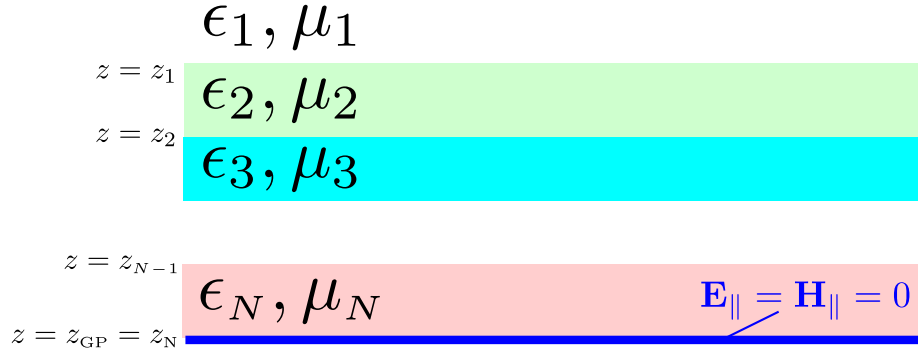


Figure 1: Geometry of the layered substrate. The n th layer has relative permittivity and permeability ϵ_n, μ_n , and its lower surface lies at $z = z_n$. The ground plane, if present, lies at $z = z_{GP}$.

1 Overview

In a previous memo¹ I considered SCUFF-STATIC electrostatics calculations in the presence of a multilayered dielectric substrate. In this memo I extend that discussion to the case of *full-wave* (i.e. nonzero frequencies beyond the quasi-static regime) scattering calculations in the SCUFF-EM core library.

Substrate geometry

As shown in Figure 1, I consider a multilayered substrate consisting of N material layers possibly terminated by a perfectly-conducting ground plane. The uppermost layer (layer 1) is the infinite half-space above the substrate. The n th layer has relative permittivity and permeability ϵ_n, μ_n , and its lower surface lies at $z = z_n$. The ground plane, if present, lies at $z \equiv z_N \equiv z_{GP}$. If the ground plane is absent, layer N is an infinite half-space.²

Definition of the substrate DGF

I will use the symbol $\mathbf{\Gamma}(\omega; \mathbf{x}_D, \mathbf{x}_S)$ for the *total* 6×6 dyadic Green's function relating time-harmonic fields at \mathbf{x}_D to sources at \mathbf{x}_S : thus, if $\mathcal{S} \equiv \begin{pmatrix} \mathbf{J} \\ \mathbf{M} \end{pmatrix}$ is the 6-vector distribution of free electric and magnetic currents in the presence of the substrate, then the 6-vector of electric and magnetic fields $\mathcal{F} \equiv \begin{pmatrix} \mathbf{E} \\ \mathbf{H} \end{pmatrix}$ is given by

$$\mathcal{F}(\mathbf{x}_D) = \int \mathbf{\Gamma}(\mathbf{x}_D, \mathbf{x}_S) \cdot \mathcal{S}(\mathbf{x}_S) d\mathbf{x}_S.$$

¹“Implicit handling of multilayered dielectric substrates in SCUFF-STATIC”

²As in the electrostatic case, this means that a finite-thickness substrate consisting of N material layers is described as a stack of $N + 1$ layers in which the bottommost layer is an infinite half-space ($z_{N+1} = -\infty$) with the material properties of vacuum ($\epsilon_{N+1} = \mu_{N+1} = 1$).

The 6×6 tensor $\mathbf{\Gamma}$ has a 2×2 block structure:

$$\mathbf{\Gamma} = \begin{pmatrix} \mathbf{\Gamma}^{\text{EE}} & \mathbf{\Gamma}^{\text{EM}} \\ \mathbf{\Gamma}^{\text{ME}} & \mathbf{\Gamma}^{\text{MM}} \end{pmatrix} \quad (1a)$$

with the 3×3 subblocks defined by

$$\Gamma_{ij}^{\text{PQ}}(\omega, \mathbf{x}_D, \mathbf{x}_S) = \begin{pmatrix} i\text{-component of P-type field at } \mathbf{x}_D \text{ due to } j\text{-directed} \\ \text{Q-type point current source at } \mathbf{x}_S, \text{ all fields and} \\ \text{sources having time dependence } \sim e^{-i\omega t} \end{pmatrix} \quad (1b)$$

Homogeneous DGF In an infinite *homogeneous* medium with relative permittivity and permeability $\{\epsilon^r, \mu^r\}$, $\mathbf{\Gamma}$ reduces to its homogeneous form, for which I will use the symbol $\mathbf{\Gamma}^{0r}$ (where the r index labels the medium, which in this case will be one of the layers in Figure 1, i.e. $r \in \{1, 2, \dots, N\}$):

$\mathbf{x}_D, \mathbf{x}_S \in \text{infinite homogeneous medium } r \implies \mathbf{\Gamma}(\omega; \mathbf{x}_D, \mathbf{x}_S) = \mathbf{\Gamma}^{0r}(\omega; \mathbf{x}_D - \mathbf{x}_S)$
where³

$$\mathbf{\Gamma}^{0r}(\omega, \mathbf{r}) \equiv \begin{pmatrix} ik_r Z_0 Z^r \mathbf{G}(k_r, \mathbf{r}) & ik_r \mathbf{C}(k_r, \mathbf{r}) \\ -ik_r \mathbf{C}(k_r, \mathbf{r}) & \frac{ik_r}{Z_0 Z^r} \mathbf{G}(k_r, \mathbf{r}) \end{pmatrix} \quad (2)$$

$$k_r \equiv \sqrt{\epsilon_0 \epsilon^r \mu_0 \mu^r} \cdot \omega, \quad Z_0 Z^r \equiv \sqrt{\frac{\mu_0 \mu^r}{\epsilon_0 \epsilon^r}},$$

$$G_{ij} = \left(\delta_{ij} - \frac{1}{k^2} \partial_i \partial_j \right) \frac{e^{ik|\mathbf{r}|}}{4\pi|\mathbf{r}|}, \quad C_{ij} = \frac{\varepsilon_{ilm}}{ik} \partial_\ell G_{mj}$$

Inhomogeneous DGF On the other hand, in the presence of the multilayered substrate the full DGF $\mathbf{\Gamma}$ receives corrections, which may be thought of as the fields radiated by surface currents induced on the interfacial surfaces of the substrate, and which I will denote by the symbol \mathcal{G} :

$$\mathbf{\Gamma}(\mathbf{x}_D, \mathbf{x}_S) = \mathcal{G}(\mathbf{x}_D, \mathbf{x}_S) + \begin{cases} \mathbf{\Gamma}^{0r}(\mathbf{x}_D - \mathbf{x}_S), & \mathbf{x}_S \in \text{layer } r \\ 0, & \text{otherwise} \end{cases} \quad (3)$$

Like $\mathbf{\Gamma}$, \mathcal{G} is a 6×6 matrix with a 2×2 block structure:

$$\mathcal{G}(\omega; \mathbf{x}_D, \mathbf{x}_S) = \begin{pmatrix} \mathcal{G}^{\text{EE}} & \mathcal{G}^{\text{EM}} \\ \mathcal{G}^{\text{ME}} & \mathcal{G}^{\text{MM}} \end{pmatrix} \quad (4)$$

with the 3×3 subblocks defined by

$$\mathcal{G}_{ij}^{\text{PQ}} = \begin{pmatrix} i\text{-component of P-type field at } \mathbf{x}_D \text{ due to surface currents on sub-} \\ \text{strate interface layers induced by } j\text{-directed Q-type source at } \mathbf{x}_S. \end{pmatrix}$$

LIBSUBSTRATE is a code for numerical computation of \mathcal{G} .

³Cf. Section 3 of the companion memo “LIBSCUFF implementation and Technical Details,” <http://homerreid.github.io/scuff-em-documentation/tex/lsInnards.pdf>

Organization of SCUFF-EM implementation and this memo

The full-wave substrate implementation in SCUFF-EM consists of multiple working parts that fit together in a somewhat modular fashion.

Roughly speaking, the computational problem may be divided into two parts:

- (a) For given source and evaluation (or “destination”) points $\{\mathbf{x}_s, \mathbf{x}_d\}$ at a given angular frequency ω in the presence of a multilayer substrate, numerically compute the substrate DGF correction $\mathcal{G}(\omega, \mathbf{x}_d, \mathbf{x}_s)$. This task is independent of SCUFF-EM and is implemented by a standalone library called LIBSUBSTRATE, described in Section 2 of this memo.
- (b) For a SCUFF-EM geometry in the presence of a substrate, compute the substrate corrections to the BEM system matrix \mathbf{M} and RHS vector \mathbf{v} , as well as the substrate corrections to post-processing quantities such as scattered fields. This is done by the file `Substrate.cc` in LIBSCUFF and is described in Section 4 of this memo.

2 Numerical computation of tensor Green's functions

In this section I discuss a method for computing the contributions of the layered substrate the *tensor* Green's function \mathcal{G} , i.e the 6×6 dyadic operator that operates on a 6-vector of electric and magnetic currents $\begin{pmatrix} \mathbf{J} \\ \mathbf{M} \end{pmatrix}$ to yield the 6-vector of electric and magnetic fields $\begin{pmatrix} \mathbf{E} \\ \mathbf{H} \end{pmatrix}$.

2.1 Overview of computational strategy

LIBSUBSTRATE decomposes the problem of computing \mathcal{G} into several logical steps, as follows:

1. Solve a linear system to obtain the Fourier-space representation $\tilde{\mathcal{G}}(\mathbf{q})$. Here $\mathbf{q} = (q_x, q_y)$ is a 2D Fourier variable. (Section 2.2.)
2. Reduce the two-dimensional integral over \mathbf{q} to a one-dimensional integral over $|\mathbf{q}| \equiv q$. (Section 2.3.)
3. Evaluate the q integral using established methods for evaluating Sommerfeld integrals. (Section ??.)

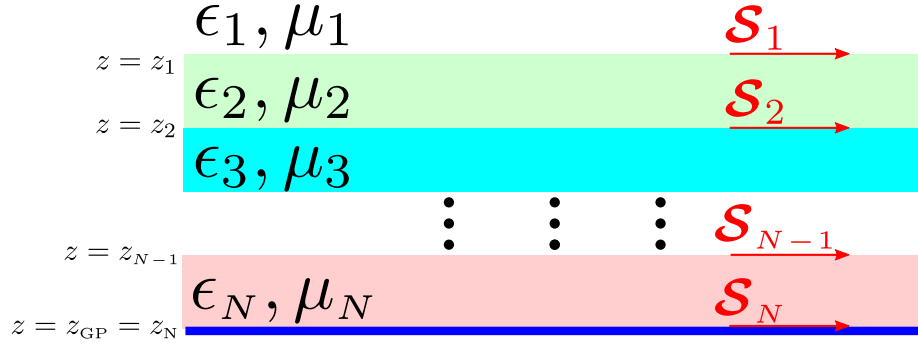


Figure 2: Effective surface-current approach to treatment of multilayer substrate. External field sources induce a distribution of electric and magnetic surface currents $\mathcal{S}_n = \begin{pmatrix} \mathbf{K}_n \\ \mathbf{N}_n \end{pmatrix}$ on the n th material interface, and the fields radiated by these effective currents account for the disturbance presented by the substrate.

2.2 Computation of Fourier-space DGF $\tilde{\mathcal{G}}(\mathbf{q})$

To compute the substrate correction to the fields of external sources, I consider the effective tangential electric and magnetic surface currents \mathbf{K} and \mathbf{N} induced on the interfacial layers by the external field sources (Figure 2). This is the direct extension to full-wave problems of the formalism I used in the electrostatic case, and it comports well with the spirit of surface-integral-equation methods.

More specifically, on the material interface layer at $z = z_n$ I have a four-vector surface-current density $\mathcal{S}_n(\boldsymbol{\rho})$, where $\boldsymbol{\rho} = (x, y)$ and the components of \mathcal{S} are

$$\mathcal{S}_n(\boldsymbol{\rho}) = \begin{pmatrix} K_x(\boldsymbol{\rho}) \\ K_y(\boldsymbol{\rho}) \\ N_x(\boldsymbol{\rho}) \\ N_y(\boldsymbol{\rho}) \end{pmatrix}. \quad (5)$$

Fields in layer interiors. I will adopt the convention that the lower (upper) bounding surface for each region is the positive (negative) bounding surface for that region in the usual sense of SCUFF-EM regions and surfaces (in which the sign of a {surface, region} pair $\{\mathcal{S}, \mathcal{R}\}$ is the sign with which surface currents on \mathcal{S} contribute to fields in \mathcal{R}). Thus, at a point $\mathbf{x} = (\boldsymbol{\rho}, z)$ in the interior of layer n ($z_{n-1} > z > z_n$), the six-vector of total fields $\mathcal{F} = \begin{pmatrix} \mathbf{E} \\ \mathbf{H} \end{pmatrix}$ reads

$$\mathcal{F}_n(\boldsymbol{\rho}, z) = -\mathbf{\Gamma}^{0n}(z_{n-1}) \star \mathcal{S}_{n-1} + \mathbf{\Gamma}^{0n}(z_n) \star \mathcal{S}_n + \mathcal{F}_n^{\text{ext}}(\boldsymbol{\rho}, z) \quad (6)$$

where $\mathcal{F}_n^{\text{ext}}$ are the externally-sourced (incident) fields due to sources in layer n , $\mathbf{\Gamma}^{0n}$ is the 6×6 homogeneous dyadic Green's function for material layer n ,

and \star is shorthand for the convolution operation

$$“\mathcal{F}(\boldsymbol{\rho}, z) \equiv \Gamma(z') \star \mathcal{S}'' \implies \mathcal{F}(\boldsymbol{\rho}, z) = \int \Gamma(\boldsymbol{\rho} - \boldsymbol{\rho}', z - z') \cdot \mathcal{S}(\boldsymbol{\rho}') d\boldsymbol{\rho}' \quad (7)$$

where the integral extends over the entire interfacial plane. I will evaluate convolutions of this form using the 2D Fourier representation of Γ^{0n} :

$$\Gamma^{0n}(\boldsymbol{\rho}, z) = \int \frac{d^2\mathbf{q}}{(2\pi)^2} \widetilde{\Gamma^{0n}}(\mathbf{q}, z) e^{i\mathbf{q} \cdot \boldsymbol{\rho}} \quad (8a)$$

$$\widetilde{\Gamma^{0n}}(\mathbf{q}, z) = \frac{1}{2} \begin{pmatrix} -\frac{\omega\mu_0\mu_n}{q_{zn}} \tilde{\mathbf{G}}^\pm & +\tilde{\mathbf{C}}^\pm \\ -\tilde{\mathbf{C}}^\pm & -\frac{\omega\epsilon_0\epsilon_n}{q_{zn}} \tilde{\mathbf{G}}^\pm \end{pmatrix} e^{iq_z|z|} \quad (8b)$$

$$\tilde{\mathbf{G}}^\pm(\mathbf{q}, k) = \begin{pmatrix} 1 & 0 & 0 \\ 0 & 1 & 0 \\ 0 & 0 & 1 \end{pmatrix} - \frac{1}{k^2} \begin{pmatrix} q_x^2 & q_x q_y & \pm q_x q_z \\ q_y q_x & q_y^2 & \pm q_y q_z \\ \pm q_z q_x & \pm q_z q_y & q_z^2 \end{pmatrix} \quad (8c)$$

$$\tilde{\mathbf{C}}^\pm(\mathbf{q}, k) = \begin{pmatrix} 0 & \mp 1 & +q_y/q_z \\ \pm 1 & 0 & -q_x/q_z \\ -q_y/q_z & +q_x/q_z & 0 \end{pmatrix} \quad (8d)$$

$$k_n \equiv \sqrt{\epsilon_0\epsilon_n\mu_0\mu_n} \cdot \omega, \quad q_z \equiv \sqrt{k^2 - |\mathbf{q}|^2}, \quad \pm = \text{sign } z. \quad (8e)$$

With this representation, convolutions like (7) become products in Fourier space:

$$\Gamma(z') \star \mathcal{S} = \mathcal{F}(\boldsymbol{\rho}, z) = \int \frac{d^2\mathbf{q}}{(2\pi)^2} \tilde{\mathcal{F}}(\mathbf{q}, z) e^{i\mathbf{q} \cdot \boldsymbol{\rho}}, \quad \text{with} \quad \tilde{\mathcal{F}}(\mathbf{q}, z) = \tilde{\Gamma}(\mathbf{q}, z - z') \tilde{\mathcal{S}}(\mathbf{q})$$

Surface currents from incident fields. To determine the surface currents induced by given incident-field sources, I apply boundary conditions. The boundary condition at $z = z_n$ is that the tangential \mathbf{E}, \mathbf{H} fields be continuous: in Fourier space, we have

$$\tilde{\mathcal{F}}_\parallel(\mathbf{q}, z = z_n^+) = \tilde{\mathcal{F}}_\parallel(\mathbf{q}, z = z_n^-) \quad (9)$$

The fields just **above** the interface ($z \rightarrow z_n^+$) receive contributions from three sources:

- Surface currents at $z = z_{n-1}$, which contribute with a minus sign and via the Green's function for region n ;
- Surface currents at $z = z_n$, which contribute with a plus sign and via the Green's function for region n ; and
- external field sources in region n .

The fields just **below** the interface ($z = z_n^-$) receive contributions from three sources:

- Surface currents at $z = z_n$, which contribute with a minus sign and via the Green's function for region $n + 1$;
- Surface currents at $z = z_{n+1}$, which contribute with a plus sign and via the Green's function for region $n + 1$; and
- external field sources in region $n + 1$.

Then equation (9) reads (temporarily omitting \mathbf{q} arguments)

$$\begin{aligned} & -\widetilde{\mathbf{\Gamma}}^{0n}_{\parallel}(z_n - z_{n-1}) \cdot \widetilde{\mathbf{S}}_{n-1} + \widetilde{\mathbf{\Gamma}}^{0n}_{\parallel}(0^+) \cdot \widetilde{\mathbf{S}}_n + \widetilde{\mathcal{F}}_{n\parallel}^{\text{ext}}(z_n) \\ & = -\widetilde{\mathbf{\Gamma}}^{0,n+1}_{\parallel}(0^-) \cdot \widetilde{\mathbf{S}}_n + \widetilde{\mathbf{\Gamma}}^{0,n+1}_{\parallel}(z_n - z_{n+1}) \cdot \widetilde{\mathbf{S}}_{n+1} + \widetilde{\mathcal{F}}_{n+1\parallel}^{\text{ext}}(z_n) \end{aligned}$$

or

$$\mathbf{M}_{n,n-1} \cdot \widetilde{\mathbf{S}}_{n-1} + \mathbf{M}_{n,n} \cdot \widetilde{\mathbf{S}}_n + \mathbf{M}_{n,n+1} \cdot \widetilde{\mathbf{S}}_{n+1} = \widetilde{\mathcal{F}}_{n+1\parallel}^{\text{ext}}(z_n) - \widetilde{\mathcal{F}}_{n\parallel}^{\text{ext}}(z_n) \quad (10)$$

with the 4×4 matrix blocks⁴

$$\mathbf{M}_{n,n-1} = -\widetilde{\mathbf{\Gamma}}^{0n}_{\parallel}(z_n - z_{n-1}) \quad (13a)$$

$$\mathbf{M}_{n,n} = +\widetilde{\mathbf{\Gamma}}^{0n}_{\parallel}(0^+) + \widetilde{\mathbf{\Gamma}}^{0,n+1}_{\parallel}(0^-) \quad (13b)$$

$$\mathbf{M}_{n,n+1} = -\widetilde{\mathbf{\Gamma}}^{0,n+1}_{\parallel}(z_n - z_{n+1}) \quad (13c)$$

Writing down equation (10) equation for all N dielectric interfaces yields a $4N \times 4N$ system of linear equations, with triadiagonal 4×4 block form, relating the surface currents on all layers to the external fields due to sources in all regions:

$$\mathbf{M} \cdot \mathbf{s} = \mathbf{f} \quad (14)$$

⁴The 4×4 \mathbf{M} blocks here have 2×2 block structure:

$$\mathbf{M}_{n,n} = \sum_{r \in \{n, n+1\}} \frac{1}{2} \begin{pmatrix} -\frac{\omega \epsilon_r}{Z_0 q_{zr}} \mathbf{g}(k_r, \mathbf{q}) & 0 \\ 0 & -\frac{\omega \mu_r Z_0}{q_{zr}} \mathbf{g}(k_r, \mathbf{q}) \end{pmatrix} \quad (11)$$

$$\mathbf{M}_{n,n\pm 1} = \frac{1}{2} \begin{pmatrix} -\frac{\omega \epsilon_r}{Z_0 q_{zr}} \mathbf{g}(k_r, \mathbf{q}) & \mathbf{c}^{\pm} \\ -\mathbf{c}^{\pm} & -\frac{\omega \mu_r Z_0}{q_{zn^*}} \mathbf{g}(k_r, \mathbf{q}) \end{pmatrix} e^{iq_{zr}|z_n - z_{n\pm 1}|} \quad (12)$$

where I put $r \equiv \begin{cases} n, & \text{for } \mathbf{M}_{n,n-1} \\ n+1, & \text{for } \mathbf{M}_{n,n+1} \end{cases}$ and

$$\mathbf{g}(k; \mathbf{q}) = \mathbf{1} - \frac{\mathbf{q}\mathbf{q}^{\top}}{k^2}, \quad \mathbf{c}^{\pm} = \begin{pmatrix} 0 & \mp 1 \\ \pm 1 & 0 \end{pmatrix}$$

where \mathbf{M} is the $4N \times 4N$ block-tridiagonal matrix (13) and where the $4N$ -vectors \mathbf{s} , \mathbf{f} read

$$\mathbf{s} = \begin{pmatrix} \tilde{\mathcal{S}}_1 \\ \tilde{\mathcal{S}}_2 \\ \tilde{\mathcal{S}}_3 \\ \vdots \\ \tilde{\mathcal{S}}_N \end{pmatrix}, \quad \mathbf{f} = \begin{pmatrix} -\tilde{\mathcal{F}}_{1\parallel}(z_1) + \tilde{\mathcal{F}}_{2\parallel}(z_1) \\ -\tilde{\mathcal{F}}_{2\parallel}(z_2) + \tilde{\mathcal{F}}_{3\parallel}(z_2) \\ -\tilde{\mathcal{F}}_{3\parallel}(z_3) + \tilde{\mathcal{F}}_{4\parallel}(z_3) \\ \vdots \\ -\tilde{\mathcal{F}}_{N-1,\parallel}(z_{N-1}) + \tilde{\mathcal{F}}_{N\parallel}(z_{N-1}) \end{pmatrix}.$$

Solving (14) yields the induced surface currents on all layers in terms of the incident fields:

$$\mathbf{s} = \mathbf{W} \cdot \mathbf{f} \quad \text{where} \quad \mathbf{W} \equiv \mathbf{M}^{-1}$$

or, more explicitly,

$$\tilde{\mathcal{S}}_n = \sum_m W_{nm} \mathbf{f}_m \quad (15)$$

Surface currents induced by point sources

For DGF computations the incident fields arise from a single point source—say, a j -directed source in region s . Then the only nonzero length-4 blocks of the RHS vector in (14) are $\mathbf{f}_{s-1}, \mathbf{f}_s$ with components ($\ell = \{1, 2, 4, 5\}$)

$$\left(\mathbf{f}_{s-1}\right)_\ell = -\tilde{\Gamma}_{\ell j}^{0s}(z_{s-1} - z_s), \quad \left(\mathbf{f}_s\right)_\ell = +\tilde{\Gamma}_{\ell j}^{0s}(z_s - z_s) \quad (16)$$

and the surface currents on interface layer n are obtained by solving (15):

$$\begin{aligned} \tilde{\mathcal{S}}_n &= \mathbf{W}_{n,s-1} \mathbf{f}_{s-1} + \mathbf{W}_{n,s} \mathbf{f}_s \\ &= \sum_{p=0}^1 (-1)^{p+1} \mathbf{W}_{n,s-1+p} \cdot \widetilde{\Gamma}_{\parallel,j}^{0s}(z_s - z_{s-1+p}) \end{aligned} \quad (17)$$

Fields due to surface currents

Given the surface currents induced by a j -directed point source at \mathbf{x}_s , I evaluate the fields due to these currents to get the substrate DGF contribution \mathcal{G} . If the evaluation point \mathbf{x}_d lies in region d , then the fields receive contributions from the surface currents at z_{d-1} and z_d , propagated by the homogeneous DGF for region d :

$$\begin{aligned} \tilde{\mathcal{F}}(z_d) &= -\widetilde{\Gamma}^{0d}(z_d - z_{d-1}) \cdot \tilde{\mathcal{S}}_{d-1} + \widetilde{\Gamma}^{0d}(z_d - z_d) \cdot \tilde{\mathcal{S}}_d \\ &= \sum_{q=0}^1 (-1)^{q+1} \widetilde{\Gamma}^{0d}(z_d - z_{d+q-1}) \cdot \tilde{\mathcal{S}}_{d+q-1} \end{aligned} \quad (18)$$

(The minus sign in the first term arises because, in my convention, surface currents on the upper surface of a region contribute to the fields in that region with a minus sign). Inserting (17), the i component here—which is the ij component of the substrate DGF—is

$$\tilde{\mathcal{G}}_{ij}(z_D, z_S) = \sum_{p,q=0}^1 (-1)^{p+q} \widetilde{\mathbf{\Gamma}^{0d}_{i,\parallel}}(z_D - z_{d-1+q}) \mathbf{W}_{d-1+q,s-1+p} \widetilde{\mathbf{\Gamma}^{0s}_{\parallel,j}}(z_{s-1+p} - z_S). \quad (19)$$

The calculation of equation (19) is carried out by the routine `GetGTwiddle` in `LIBSUBSTRATE`.

2.3 Reduction of 2D Fourier integrals to 1D (Sommerfeld) integrals

The real-space DGF correction is the inverse Fourier transform of (19):

$$\mathcal{G}(\boldsymbol{\rho}, z_D, z_S) = \int \frac{d^2 \mathbf{q}}{(2\pi)^2} \tilde{\mathcal{G}}(\mathbf{q}; z_D; z_S) e^{i\mathbf{q} \cdot \boldsymbol{\rho}}$$

or, in polar coordinates with $(q_x, q_y) = (q \cos \theta_q, q \sin \theta_q)$, $(\rho_x, \rho_y) = (\rho \cos \theta_\rho, \rho \sin \theta_\rho)$,

$$\mathcal{G}(\boldsymbol{\rho}) = \int_0^\infty \frac{q dq}{2\pi} \int_0^{2\pi} \frac{d\theta_q}{2\pi} \tilde{\mathcal{G}}(\mathbf{q}) e^{iq\rho \cos(\theta_q - \theta_\rho)}. \quad (20)$$

(Here and for much of this section I suppress $z_{D,S}$ arguments, but one must remember that they are always there.⁵) The goal of this section is to integrate out the angular variable θ_q to reduce the 2D integral over \mathbf{q} to a 1D integral over $q = |\mathbf{q}|$. In abbreviated form this proceeds as follows:

1. Separate variables by writing $\tilde{\mathcal{G}}(\mathbf{q})$ as a sum of products of θ_q -independent scalar functions $\tilde{g}(q)$ times q -independent matrix-valued functions $\mathbf{\Lambda}(\theta_q)$ (Section 2.3.1):

$$\tilde{\mathcal{G}}(\mathbf{q}) = \sum_{n=1}^{18} \tilde{g}^{(n)}(q) \mathbf{\Lambda}^{(n)}(\theta_q)$$

2. Evaluate integrals over θ_q analytically to yield Bessel functions $J_\nu(q\rho)$ multiplying q -independent matrix-valued functions $\mathbf{\Lambda}(\theta_\rho)$ (Section 2.3.2). After this step (20) reads

$$\mathcal{G}(\boldsymbol{\rho}) = \sum_{m=1}^{22} \underbrace{\left[\int_0^\infty \tilde{\mathbf{g}}^{(m)}(q, \rho) dq \right]}_{\mathbf{g}^{(m)}(\rho)} \mathbf{\Lambda}^{(m)}(\theta_\rho) \quad (21)$$

where the $\tilde{\mathbf{g}}(q, \rho)$ functions are linear combinations of the $\tilde{g}(q)$ functions times Bessel functions in $q\rho$ and other factors.

3. Evaluate the remaining integrals over q numerically using sophisticated tricks for evaluating Sommerfeld integrals (Section 2.3.3).

2.3.1 Factor $\tilde{\mathcal{G}}$ into q -independent and θ_q -independent terms

I begin by noting that $\tilde{\mathcal{G}}(\mathbf{q})$ may be decomposed as a sum of scalar functions of $q = |\mathbf{q}|$ times q -independent matrix-valued functions of θ_q :

$$\tilde{\mathcal{G}}(\mathbf{q}) = \sum_{n=1}^{18} \tilde{g}^{(n)}(q) \mathbf{\Lambda}^{(n)}(\theta_q) \quad (22)$$

⁵More specifically, the “ g -like” quantities $\mathcal{G}(\boldsymbol{\rho})$, $\tilde{\mathcal{G}}(\mathbf{q})$, $\tilde{g}(q)$, $\tilde{\mathbf{g}}(q, \rho)$, and $\mathbf{g}(\rho)$ all depend on $z_{S,D}$, but the matrix-valued functions $\mathbf{\Lambda}_n(\theta)$ do not.

For example, the upper two quadrants read

$$\begin{aligned}
\widetilde{\mathcal{G}}^{\text{EE}}(\mathbf{q}) = & \underbrace{\widetilde{g}^{\text{EE}0\parallel}(q) \begin{pmatrix} 1 & 0 & 0 \\ 0 & 1 & 0 \\ 0 & 0 & 0 \end{pmatrix}}_{\mathbf{\Lambda}^{0\parallel}} + \underbrace{\widetilde{g}^{\text{EE}0z}(q) \begin{pmatrix} 0 & 0 & 0 \\ 0 & 0 & 0 \\ 0 & 0 & 1 \end{pmatrix}}_{\mathbf{\Lambda}^{0z}} \\
& + \underbrace{\widetilde{g}^{\text{EE}1}(q) \begin{pmatrix} 0 & 0 & \cos \theta_{\mathbf{q}} \\ 0 & 0 & \sin \theta_{\mathbf{q}} \\ 0 & 0 & 0 \end{pmatrix}}_{\mathbf{\Lambda}^1(\theta_{\mathbf{q}})} + \underbrace{\widetilde{g}^{\text{EE}1\top}(q) \begin{pmatrix} 0 & 0 & 0 \\ 0 & 0 & 0 \\ \cos \theta_{\mathbf{q}} & \sin \theta_{\mathbf{q}} & 0 \end{pmatrix}}_{\mathbf{\Lambda}^{1\top}(\theta_{\mathbf{q}})} \\
& + \underbrace{\widetilde{g}^{\text{EE}2}(q) \begin{pmatrix} \cos^2 \theta_{\mathbf{q}} & \cos \theta_{\mathbf{q}} \sin \theta_{\mathbf{q}} & 0 \\ \cos \theta_{\mathbf{q}} \sin \theta_{\mathbf{q}} & \sin^2 \theta_{\mathbf{q}} & 0 \\ 0 & 0 & 0 \end{pmatrix}}_{\mathbf{\Lambda}^2(\theta_{\mathbf{q}})} \\
\widetilde{\mathcal{G}}^{\text{EM}}(\mathbf{q}) = & \underbrace{\widetilde{g}^{\text{EM}0\parallel}(q) \begin{pmatrix} 0 & 1 & 0 \\ -1 & 0 & 0 \\ 0 & 0 & 0 \end{pmatrix}}_{\mathbf{\Lambda}^{0\times}} + \underbrace{\widetilde{g}^{\text{EM}2}(q) \begin{pmatrix} \cos \theta_{\mathbf{q}} \sin \theta_{\mathbf{q}} & \sin^2 \theta_{\mathbf{q}} & 0 \\ -\cos^2 \theta_{\mathbf{q}} & -\cos \theta_{\mathbf{q}} \sin \theta_{\mathbf{q}} & 0 \\ 0 & 0 & 0 \end{pmatrix}}_{\mathbf{\Lambda}^{2\times}} \\
& + \underbrace{\widetilde{g}^{\text{EM}1}(q) \begin{pmatrix} 0 & 0 & -\sin \theta_{\mathbf{q}} \\ 0 & 0 & +\cos \theta_{\mathbf{q}} \\ 0 & 0 & 1 \end{pmatrix}}_{\mathbf{\Lambda}^{1\times}} + \underbrace{\widetilde{g}^{\text{EM}1\top}(q) \begin{pmatrix} 0 & 0 & 0 \\ 0 & 0 & 0 \\ -\sin \theta_{\mathbf{q}} & \cos \theta_{\mathbf{q}} & 1 \end{pmatrix}}_{\mathbf{\Lambda}^{1\times\top}}
\end{aligned}$$

where the \top superscript indicates matrix transpose. The expressions for $\widetilde{\mathcal{G}}^{\text{ME}}$ and $\widetilde{\mathcal{G}}^{\text{MM}}$ are similar, involving the same $\mathbf{\Lambda}$ matrices with different \widetilde{g} prefactors.

2.3.2 Evaluate $\theta_{\mathbf{q}}$ integrals

Using Table 3, the $\theta_{\mathbf{q}}$ integral in (20) may be evaluated analytically to yield Bessel-function factors $J_{\nu}(q\rho)$ ($\nu \in \{0, 1, 2\}$) times $\mathbf{\Lambda}$ matrices, now evaluated

$$\frac{1}{2\pi} \int_0^{2\pi} e^{iq\rho \cos(\theta_q - \theta_\rho)} \begin{pmatrix} 1 \\ \cos \theta_q \\ \sin \theta_q \\ \cos^2 \theta_q \\ \cos \theta_q \sin \theta_q \\ \sin^2 \theta_q \end{pmatrix} d\theta_q = \begin{pmatrix} J_0(q\rho) \\ iJ_1(q\rho) \cos \theta_\rho \\ iJ_1(q\rho) \sin \theta_\rho \\ -J_2(q\rho) \cos^2 \theta_\rho + \frac{J_1(q\rho)}{q\rho} \\ -J_2(q\rho) \cos \theta_\rho \sin \theta_\rho \\ -J_2(q\rho) \sin^2 \theta_\rho + \frac{J_1(q\rho)}{q\rho} \end{pmatrix},$$

Figure 3: Table of integrals used to reduce 2D integrals over \mathbf{q} to 1D integrals over $|q|$.

at θ_ρ . For example, one term in the expansion of $\mathcal{G}(\rho)$ is

$$\begin{aligned} & \int_0^\infty \frac{q dq}{2\pi} \tilde{g}^{\text{EE1}}(q) \underbrace{\int_0^{2\pi} \frac{d\theta_q}{2\pi} \Lambda^1(\theta_q) e^{iq\rho \cos(\theta_q - \theta_\rho)}}_{iJ_1(q\rho) \Lambda^1(\theta_\rho)} \\ &= \underbrace{\left\{ \int_0^\infty dq \underbrace{\left[\frac{q}{2\pi} \tilde{g}^{\text{EE1}}(q) \cdot iJ_1(q\rho) \right]}_{\tilde{\mathfrak{g}}^{\text{EE1}}(q, \rho)} \right\}}_{\mathfrak{g}^{\text{EE1}}(\rho)} \Lambda^1(\theta_\rho) \end{aligned}$$

The second line here defines some new symbols: $\tilde{\mathfrak{g}}$ are functions of q and ρ defined as products of $\tilde{g}(q)$ factors times $J_\nu(q\rho)$ factors and other factors, while \mathfrak{g} are functions of ρ obtained by integrating out the q dependence of $\mathfrak{g}(q, \rho)$. The

full set of rules defining the $\tilde{\mathfrak{g}}$ is

$$\tilde{\mathfrak{g}}^{\text{EE0}\parallel}(q, \rho) \equiv \frac{q}{2\pi} \left[\tilde{g}^{\text{EE0}\parallel}(q) J_0(q\rho) + \tilde{g}^{\text{EE2}}(q) \frac{J_1(q\rho)}{q\rho} \right] \quad (23a)$$

$$\tilde{\mathfrak{g}}^{\text{EE0}z}(q, \rho) \equiv \frac{q}{2\pi} \tilde{g}^{\text{EE0}z}(q) J_0(q\rho) \quad (23b)$$

$$\tilde{\mathfrak{g}}^{\text{EE1}}(q, \rho) \equiv i \frac{q}{2\pi} \tilde{g}^{\text{EE1}}(q) J_1(q\rho) \quad (23c)$$

$$\tilde{\mathfrak{g}}^{\text{EE1}\top}(q, \rho) \equiv i \frac{q}{2\pi} \tilde{g}^{\text{EE1}\top}(q) J_1(q\rho) \quad (23d)$$

$$\tilde{\mathfrak{g}}^{\text{EE2}}(q, \rho) \equiv -\frac{q}{2\pi} \tilde{g}^{\text{EE2}}(q) J_2(q\rho) \quad (23e)$$

$$\tilde{\mathfrak{g}}^{\text{EM0}\parallel \times}(q, \rho) \equiv \frac{q}{2\pi} \left[\tilde{g}^{\text{EM0}\parallel}(q) J_0(q\rho) + \tilde{g}^{\text{EM2}}(q) \frac{J_1(q\rho)}{q\rho} \right] \quad (23f)$$

$$\tilde{\mathfrak{g}}^{\text{EM1}\times}(q, \rho) \equiv i \frac{q}{2\pi} \tilde{g}^{\text{EM1A}}(q) J_1(q\rho) \quad (23g)$$

$$\tilde{\mathfrak{g}}^{\text{EM1}\times\top}(q, \rho) \equiv i \frac{q}{2\pi} \tilde{g}^{\text{EM1B}}(q) J_1(q\rho) \quad (23h)$$

$$\tilde{\mathfrak{g}}^{\text{EM2}\times}(q, \rho) \equiv -\frac{q}{2\pi} \tilde{g}^{\text{EM2}} J_2(q\rho) \quad (23i)$$

2.3.3 Evaluate Sommerfeld integrals over q

Assembling the above pieces, the substrate DGF correction \mathcal{G} is a sum of 22 terms:⁶

$$\mathcal{G}(\rho) = \sum_{m=1}^{22} \mathfrak{g}^{(m)}(\rho) \Lambda^{(m)}(\theta_\rho),$$

where the $\mathfrak{g}^{(m)}(\rho)$ functions are defined by Sommerfeld integrals:

$$\mathfrak{g}^{(m)}(\rho) \equiv \int_0^\infty \tilde{\mathfrak{g}}^{(m)}(q, \rho) dq. \quad (24)$$

⁶This tally treats the integrals of the two integrand terms on the RHS of (23a) as two separate integrals [and similarly for (23f) and the corresponding equations for the ME and MM quadrants]. If the terms are lumped together then the number of distinct \mathfrak{g} functions is 18.

3 Numerical computation of scalar Green's functions

An alternative to computing the 6×6 tensor Green's function is instead to consider the 4 *scalar* Green's functions that give the electric and magnetic scalar and vector potentials due to electric and magnetic current and charge distributions.

In this approach we think of currents and charge densities as separate, independent types of sources, which give rise respectively to vector and scalar potentials. More specifically, an electric current distribution $\mathbf{J}(\mathbf{x})$

Of course, in reality

In equation (18) I am computing the 6 components of the \mathbf{E} and \mathbf{H} fields produced by the induced surface currents. If instead I compute the *potentials* produced by those currents I obtain a slightly different Green's function. Thus, let \mathbf{A}^E, Φ^E be the usual vector and scalar potential of an electric-current source in a homogeneous region, and let \mathbf{A}^M, Φ^M be their counterparts for magnetic-current sources, i.e. if the electric and magnetic volume currents are \mathbf{J} and \mathbf{M} then

$$\mathbf{A}^E(\mathbf{x}_D) = \int \mathbf{J}(\mathbf{x}_S) G_0(\mathbf{x}_{DS}) d\mathbf{x}_S, \quad \Phi^E(\mathbf{x}_D) = \frac{1}{i\omega\epsilon} \int (\nabla \cdot \mathbf{J}) G_0(\mathbf{x}_{DS}) d\mathbf{x}_S \quad (25a)$$

$$\mathbf{A}^M(\mathbf{x}_D) = \epsilon \int \mathbf{M}(\mathbf{x}_S) G_0(\mathbf{x}_{DS}) d\mathbf{x}_S, \quad \Phi^M(\mathbf{x}_D) = \frac{1}{i\omega\mu} \int (\nabla \cdot \mathbf{M}) G_0(\mathbf{x}_{DS}) d\mathbf{x}_S \quad (25b)$$

with $\mathbf{x}_{DS} \equiv \mathbf{x}_D - \mathbf{x}_S$ and

$$G_0(k; \mathbf{r}) = \frac{e^{ik|\mathbf{r}|}}{4\pi|\mathbf{r}|} = \int \frac{d^2\mathbf{q}}{(2\pi)^2} \tilde{G}_0(\mathbf{q}, z) e^{i\mathbf{q} \cdot \boldsymbol{\rho}}, \quad \tilde{G}_0 = \frac{i}{2q_z} e^{iq_z|z|}.$$

4 SCUFF-EM integration: Substrate contributions to BEM matrix and RHS vector

4.1 Fields of individual basis functions

$$\mathcal{G}^{\text{EE}} =$$

4.2 SIE matrix elements: Panel-panel integrals

If $\mathcal{S}_\alpha, \mathcal{S}_\beta$ are two `RWGSurfaces` exposed to the outermost (ambient) region in a SCUFF-EM geometry, then the elements of the SIE matrix elements corresponding to any pair of basis functions $\{\mathbf{b}_a \in \mathcal{S}_\alpha, \mathbf{b}_b \in \mathcal{S}_\beta\}$ receive corrections of the form

$$\begin{aligned} \Delta M_{ab}^{\text{PQ}} &= \langle \mathbf{b}_a | \mathcal{G}^{\text{PQ}} | \mathbf{b}_b \rangle \\ &\equiv \iint \mathbf{b}_a(\mathbf{x}_a) \cdot \mathcal{G}^{\text{PQ}}(\mathbf{x}_a, \mathbf{x}_b) \cdot \mathbf{b}_b(\mathbf{x}_b) d\mathbf{x}_b d\mathbf{x}_a \end{aligned} \quad (26)$$

I will consider two different approaches for evaluating the panel-panel integrals⁷ here:

1. The *spectral inner* approach: In this case I simply evaluate the panel-panel cubature in (26), with values of \mathcal{G} at each cubature point computed via the methods of `LIBSUBSTRATE` as described in the previous section (possibly accelerated via interpolation tables). I call this the “spectral inner” method because in this case the q integral in the definition of \mathcal{G} is the innermost of 3 integrals. Indeed, inserting equation (21) we have

$$\begin{aligned} \Delta M_{ab}^{\text{PQ}} &\equiv \iint \mathbf{b}_a(\mathbf{x}_a) \left\{ \sum \mathfrak{g}^{(m)}(\rho) \mathbf{\Lambda}^{(m)}(\theta_\rho) \right\} \mathbf{b}_b(\mathbf{x}_b) d\mathbf{x}_b d\mathbf{x}_a \\ &\quad \text{[where } \boldsymbol{\rho} = (\mathbf{x}_a - \mathbf{x}_b)_\parallel = (\rho \cos \theta_\rho, \rho \sin \theta_\rho)\text{]. Recalling the definition (24),} \\ &\quad \text{this is a sum of triple integrals:} \\ &\equiv \iint \mathbf{b}_a(\mathbf{x}_a) \left\{ \sum \left[\int_0^\infty \tilde{\mathfrak{g}}^{(m)}(q, \rho) dq \right] \mathbf{\Lambda}^{(m)}(\theta_\rho) \right\} \cdot \mathbf{b}_b(\mathbf{x}_b) d\mathbf{x}_b d\mathbf{x}_a. \end{aligned} \quad (27)$$

2. The *spectral outer* approach: In this case I rearrange the order of integration in (28) so that the q integral is the *outermost* integral, with an integrand defined for each q by a panel-panel integral involving the spectral-domain GF:

$$\Delta M_{ab}^{\text{PQ}} = \int_0^\infty \left\{ \iint \mathbf{b}_a(\mathbf{x}_a) \left[\sum \tilde{\mathfrak{g}}^{(m)}(q, \rho) \mathbf{\Lambda}^{(m)}(\theta_\rho) \right] \mathbf{b}_b(\mathbf{x}_b) d\mathbf{x}_b d\mathbf{x}_a \right\} dq \quad (28)$$

⁷I refer to 4-dimensional integrals like (26) as “panel-panel integrals” because they are a sum of contributions of integrals over pairs of flat triangular panels.

$$\mathcal{G}_{ij}^{\text{EE}} = \delta_{ij}$$

5 Metal-on-Insulator geometries

$$\begin{aligned}\mathbf{E} &= iw\mathbf{A} - \nabla\phi \\ &= iw\mu G_0 \star \mathbf{J} - \frac{1}{i\omega\epsilon} \nabla G_0 \star \rho\end{aligned}$$

$$\begin{aligned}\tilde{G}^{\text{App}} &= \frac{1}{2\pi} q J_0(q\rho) \zeta^{\text{App}} \\ \tilde{G}^{\text{Apz}} &= -\frac{1}{2\pi} (\epsilon_r - 1) q^2 J_1(q\rho) \zeta^{\text{Apz}} \\ \tilde{G}^{\Phi} &= \frac{1}{2\pi} \rho J_0(q\rho) \zeta^{\Phi}\end{aligned}$$

$$\begin{aligned}\zeta^{\text{App}} &= \frac{1}{D^{\text{TE}}} \times \left\{ \frac{e^{-u_0 z}}{\frac{\sinh u(z+h)}{\sinh uh}} \right. \\ \zeta^{\text{Apz}} &= \frac{1}{D^{\text{TE}} D^{\text{TM}}} \times \left\{ \frac{e^{-u_0 z}}{\frac{\cosh u(z+h)}{\cosh uh}} \right. \\ \zeta^{\Phi} &= \frac{N}{D^{\text{TE}} D^{\text{TM}}} \times \left\{ \frac{e^{-u_0 z}}{\frac{\sinh u(z+h)}{\sinh uh}} \right.\end{aligned}$$

$$\frac{N}{D^{\text{TE}} D^{\text{TM}}} \xrightarrow{u \rightarrow u_0} \frac{1 - e^{-2u_0 h}}{u_0(\epsilon + 1)} \sum_{n=0}^{\infty} \left[-\eta e^{-2u_0 h} \right]^n$$

6 Unit-test framework

The LIBSUBSTRATE standalone library comes with a unit-test suite to test core functionality related to calculation of substrate DGFs. Separately, the unit-test suite for LIBSCUFF includes tests to check the integration of LIBSUBSTRATE into LIBSCUFF.

6.1 LIBSUBSTRATE unit tests

6.1.1 tGTwiddle

The unit-test code `tGTwiddle.cc` tests that the full Fourier-space DGF $\tilde{\Gamma}(\mathbf{q}, z_D, z_S)$ satisfies the appropriate boundary conditions at each layer of the layered substrate, namely

$$C^+(P, i, \ell) \tilde{\Gamma}_{ij}^{\text{PQ}}(\mathbf{q}, z_\ell + \eta, z_S) C^-(P, i, \ell) \tilde{\Gamma}_{ij}^{\text{PQ}}(\mathbf{q}, z_\ell - \eta, z_S) \quad (29)$$

where

$$C^\pm(P, i, \ell) = \begin{cases} 1, & i \in \{x, y\} \\ \epsilon_\ell^\pm, & i = z, P = E \\ \mu_\ell^\pm, & i = z, P = H \end{cases}$$

where $\{\epsilon, \mu\}_\ell^\pm$ are the material properties for the layer above/below z_ℓ , i.e. (Figure ??)

$$\{\epsilon_\ell, \mu_\ell\}^+ = \{\epsilon_\ell, \mu_\ell\}, \quad \{\epsilon_\ell, \mu_\ell\}^- = \{\epsilon_{\ell+1}, \mu_{\ell+1}\}.$$

If a ground plane is present, we have the additional condition

$$\tilde{\Gamma}_{ij}^{\text{PQ}}(q, z_{\text{GP}}, z_S) = 0 \quad \text{for } i \in \{x, y\}. \quad (30)$$

Conditions (29) and (30) must hold *independently* of the indices $Q \in \{E, H\}$ and $j \in \{1, 2, 3\}$ and of the values of \mathbf{q} and z_S .

A Symbols and indices used in this document

A.1 Symbols

Symbol	Arguments	Description
\mathcal{F}	\mathbf{r} , geometry	Field six-vector $\mathcal{F} = \begin{pmatrix} \mathbf{E} \\ \mathbf{H} \end{pmatrix}$
\mathcal{C}	\mathbf{r} , geometry	Current six-vector $\mathcal{C} = \begin{pmatrix} \mathbf{J} \\ \mathbf{M} \end{pmatrix}$ or $\mathcal{C} = \begin{pmatrix} \mathbf{K} \\ \mathbf{N} \end{pmatrix}$
$\mathbf{\Gamma}$	$\boldsymbol{\rho}$, z_D , z_S , ω , geometry	Full (bare+scattered) 6×6 dyadic Green's function, $\mathcal{F} = \mathbf{\Gamma} \star \mathcal{C}$
$\mathbf{\Gamma}^{0r}$	$\boldsymbol{\rho}$, z_D , z_S , ω , ϵ^r , μ^r	Bare (homogeneous) 6×6 dyadic Green's function in region r
\mathcal{G}	$\boldsymbol{\rho}$, z_D , z_S , ω , geometry	Scattering contribution to $\mathbf{\Gamma}$ ($\mathbf{\Gamma} = \mathbf{\Gamma}^{0r} + \mathcal{G}$)
\mathcal{P}	\mathbf{r} , geometry	Potential eight-vector $\mathcal{P} = \begin{pmatrix} \mathbf{A}^E \\ \Phi^E \\ \mathbf{A}^M \\ \Phi^M \end{pmatrix}$
\mathcal{S}	\mathbf{r} , geometry	Source eight-vector $\mathcal{S} = \begin{pmatrix} \mathbf{J} \\ \rho^E \\ \mathbf{M} \\ \rho^M \end{pmatrix}$
$\mathbf{\Lambda}$	$\boldsymbol{\rho}$, z_D , z_S , ω , geometry	Full (bare+scattered) 8×8 dyadic Green's function, $\mathcal{P} = \mathbf{\Lambda} \star \mathcal{S}$
$\mathbf{\Lambda}^{0r}$	$\boldsymbol{\rho}$, z_D , z_S , ω , geometry	Bare (homogeneous) 8×8 dyadic Green's function for region r
\mathcal{L}	$\boldsymbol{\rho}$, z_D , z_S , ω , geometry	Scattering contribution to $\mathbf{\Lambda}$ ($\mathbf{\Lambda} = \mathbf{\Lambda}^{0r} + \mathcal{L}$)

A.2 Indices

Index	Range	Significance								
i, j	$\{1, 2, 3\}$	Cartesian directions x, y, z								
I, J	$\{1, 2, 3, 4, 5, 6\}$	Electric/magnetic field/current components <table><tr><td>1,2,3</td><td>$E_{x,y,z}, J_{x,y,z}, K_{x,y,z}$</td></tr><tr><td>4,5,6</td><td>$H_{x,y,z}, M_{x,y,z}, N_{x,y,z}$</td></tr></table>	1,2,3	$E_{x,y,z}, J_{x,y,z}, K_{x,y,z}$	4,5,6	$H_{x,y,z}, M_{x,y,z}, N_{x,y,z}$				
1,2,3	$E_{x,y,z}, J_{x,y,z}, K_{x,y,z}$									
4,5,6	$H_{x,y,z}, M_{x,y,z}, N_{x,y,z}$									
μ, ν	$\{1, 2, 3, 4, 5, 6, 7, 8\}$	Electric/magnetic potential/source components <table><tr><td>1,2,3</td><td>$A^{\text{E}}_{x,y,z}, J_{x,y,z}, K_{x,y,z}$</td></tr><tr><td>4</td><td>$\Phi^{\text{E}}, \rho^{\text{E}}, \sigma^{\text{E}}$</td></tr><tr><td>5,6,7</td><td>$A^{\text{M}}_{x,y,z}, M_{x,y,z}, N_{x,y,z}$</td></tr><tr><td>8</td><td>$\Phi^{\text{M}}, \rho^{\text{M}}, \sigma^{\text{M}}$</td></tr></table>	1,2,3	$A^{\text{E}}_{x,y,z}, J_{x,y,z}, K_{x,y,z}$	4	$\Phi^{\text{E}}, \rho^{\text{E}}, \sigma^{\text{E}}$	5,6,7	$A^{\text{M}}_{x,y,z}, M_{x,y,z}, N_{x,y,z}$	8	$\Phi^{\text{M}}, \rho^{\text{M}}, \sigma^{\text{M}}$
1,2,3	$A^{\text{E}}_{x,y,z}, J_{x,y,z}, K_{x,y,z}$									
4	$\Phi^{\text{E}}, \rho^{\text{E}}, \sigma^{\text{E}}$									
5,6,7	$A^{\text{M}}_{x,y,z}, M_{x,y,z}, N_{x,y,z}$									
8	$\Phi^{\text{M}}, \rho^{\text{M}}, \sigma^{\text{M}}$									

B 8×8 Dyadic Green's Functions

The usual 6×6 dyadic Green's function $\mathbf{\Gamma}$ operates on a six-vector of currents to yield a six-vector of fields. It is convenient to consider a slightly different object that operates on an *eight*-vector of sources to yield an *eight*-vector of potentials.

In the presence of magnetic currents, the usual (electric-current-sourced) vector and scalar potentials \mathbf{A}^E, Φ^E , are joined by their magnetic-current-sourced counterparts \mathbf{A}^M, Φ^M , which are related to the fields according to

$$\begin{aligned}\mathbf{E} &= i\omega\mu\mathbf{A}^E - \frac{1}{i\omega\epsilon}\nabla\Phi^E - \nabla \times \mathbf{A}^M \\ \mathbf{M} &= \nabla \times \mathbf{A}^E + i\omega\epsilon\mathbf{A}^M - \frac{1}{i\omega\mu}\nabla\Phi^M.\end{aligned}$$

In a homogeneous region, the potentials⁸ produced by given source distributions $\{\mathbf{J}, \mathbf{M}\}$ are

$$\begin{aligned}\mathbf{A}^E(\mathbf{x}_D) &= \int G_0(\mathbf{x}_D - \mathbf{x}_S) \mathbf{J}(\mathbf{x}_S) d\mathbf{x}_S, & \Phi^E(\mathbf{x}_D) &= \int G_0(\mathbf{x}_D - \mathbf{x}_S) [\nabla \cdot \mathbf{J}] d\mathbf{x}_S \\ \mathbf{A}^M(\mathbf{x}_D) &= \int G_0(\mathbf{x}_D - \mathbf{x}_S) \mathbf{M}(\mathbf{x}_S) d\mathbf{x}_S, & \Phi^M(\mathbf{x}_D) &= \int G_0(\mathbf{x}_D - \mathbf{x}_S) [\nabla \cdot \mathbf{M}] d\mathbf{x}_S\end{aligned}$$

where

$$G_0(\mathbf{r}) = \frac{e^{ik|\mathbf{r}|}}{4\pi|\mathbf{r}|}.$$

$$\begin{pmatrix} E_x \\ E_y \\ E_z \\ H_x \\ H_y \\ H_z \end{pmatrix} = \begin{pmatrix} i\omega\mu G_0 & 0 & 0 & -\frac{1}{i\omega\epsilon}\partial_x G_0 & 0 & \partial_z G_0 & -\partial_y G_0 & 0 \\ 0 & i\omega\mu G_0 & 0 & -\frac{1}{i\omega\epsilon}\partial_y G_0 & -\partial_z G_0 & 0 & \partial_x G_0 & 0 \\ 0 & 0 & i\omega\mu G_0 & -\frac{1}{i\omega\epsilon}\partial_z G_0 & \partial_y G_0 & -\partial_x G_0 & 0 & 0 \\ 0 & -\partial_z G_0 & \partial_y G_0 & 0 & i\omega\epsilon G_0 & 0 & 0 & -\frac{1}{i\omega\mu}\partial_x G_0 \\ \partial_z G_0 & 0 & \partial_x G_0 & 0 & 0 & i\omega\epsilon G_0 & 0 & -\frac{1}{i\omega\mu}\partial_y G_0 \\ -\partial_y G_0 & \partial_x G_0 & 0 & 0 & 0 & 0 & i\omega\epsilon G_0 & -\frac{1}{i\omega\mu}\partial_z G_0 \end{pmatrix} \star \begin{pmatrix} J_x \\ J_y \\ J_z \\ \nabla \cdot \mathbf{J} \\ M_x \\ M_y \\ M_z \\ \nabla \cdot \mathbf{M} \end{pmatrix}$$

⁸Note that my $\Phi^{E,M}$ are $i\omega\{\epsilon, \mu\}$ times the actual scalar potentials due to the charge distributions associated with currents \mathbf{J}, \mathbf{M} .

C Analytical result for single material interface in the low-frequency or short-distance limits

For the case of just a single material interface with no ground plane—i.e. the substrate is an infinite half-space—the DGF calculation simplifies enough to allow analytical evaluation in the low-frequency and/or short-distance limits.

In this case, the 4×4 system of equations (??) relating induced surface currents to incident fields in Fourier space splits into two disconnected 2×2 blocks:

$$\begin{pmatrix} \mathbf{M}^E & 0 \\ 0 & \mathbf{M}^M \end{pmatrix} \begin{pmatrix} \widetilde{k_x} \\ \widetilde{k_y} \\ \widetilde{n_x} \\ \widetilde{n_y} \end{pmatrix} = - \begin{pmatrix} \widetilde{e_x} \\ \widetilde{e_y} \\ \widetilde{h_x} \\ \widetilde{h_y} \end{pmatrix} \quad (31)$$

where the matrix blocks have the structure ($P = \{E, M\}$)

$$M_{ij}^P = f_1^P \delta_{ij} + f_2^P \frac{q_i q_j}{q^2}$$

with

$$f_1^E = -\frac{\omega}{2} \left[\frac{\mu^A}{q_z^A} + \frac{\mu^B}{q_z^B} \right], \quad f_2^E = +\frac{q^2}{2\omega} \left[\frac{1}{\epsilon^A q_z^A} + \frac{1}{\epsilon^B q_z^B} \right]$$

and f_{12}^M similar with $\epsilon \leftrightarrow \mu$. Considering an ansatz for the inverse $\mathbf{W} = \mathbf{M}^{-1}$ of the form

$$W_{ij}^P = g_1^P \delta_{ij} + g_2^P \frac{q_i q_j}{q^2} \quad (32)$$

and demanding $\mathbf{M}\mathbf{W} = \mathbf{1}$ yields

$$g_1 = \frac{1}{f_1}, \quad g_2 = -\frac{f_2}{f_1(f_1 + f_2)}. \quad (33)$$

For a j -directed point electric source of strength \mathcal{J} at a distance z_s above the interface [that is, a pointlike current distribution $\mathbf{J}(\mathbf{x}) = \mathcal{J} \hat{\mathbf{r}}_j \delta(\mathbf{x} - \mathbf{x}_s)$ with $x_s = (0, 0, z_s)$] the tangential fields that enter the RHS of (??) are

$$\begin{pmatrix} \widetilde{e_x} \\ \widetilde{e_y} \\ \widetilde{h_x} \\ \widetilde{h_y} \end{pmatrix} = \frac{\mathcal{J}}{2q_z^A} \begin{pmatrix} -\omega\mu^A\delta_{jx} + \frac{q_x q_j}{\omega\epsilon^A} \\ -\omega\mu^A\delta_{jy} + \frac{q_y q_j}{\omega\epsilon^A} \\ -q_y\delta_{jz} + q_z^A\delta_{jy} \\ +q_x\delta_{jy} - q_z^A\delta_{jx} \end{pmatrix} \quad (34)$$

Armed with (??), (??), and (??), I can now obtain analytical formulas for the Fourier-space surface currents—but unfortunately the results are too unwieldy to be useful in practice.

To make progress, I make the following simplifications:

- I put $q_z^B = q_z^A$. The rationale is that I am interested in the behavior as $q \rightarrow \infty$, in which case q_z^B does become equal to q_z^A .

- I consider the nonmagnetic case $\mu^{\text{A}} = \mu^{\text{B}} = 1$.

With these simplifications, the components of the induced surface currents on the interface read

$$\frac{\tilde{k}_i}{\mathcal{J}} = -\delta_{ij} - \frac{\epsilon^{\text{B}}}{\epsilon^{\text{A}}} \frac{q_i q_j}{q^2 - \epsilon^{\text{P}} \omega^2}, \quad \frac{\tilde{n}_i}{\mathcal{J}} = \varepsilon_{ij} \frac{\omega q_z}{q^2} + \frac{q^2 q_z}{\omega \epsilon^{\text{S}} [q^2 - \epsilon^{\text{S}} \omega^2]} - \dots$$